Case Studies in Thermal Engineering 59 (2024) 104491

Contents lists available at ScienceDirect

Case Studies in Thermal Engineering

journal homepage: www.elsevier.com/locate/csite

Occupant's thermal comfort augmentation and thermal load reduction in a typical residential building using genetic algorithm

Mohammadreza Baghoolizadeh [a,*], Mahmoud Behzadi Hamooleh [a], As'ad Alizadeh [b,**], Amir Torabi [a], Dheyaa J. Jasim [c], Mohammad Rostamzadeh-Renani [d], Reza Rostamzadeh-Renani [d]

[a] Department of Mechanical Engineering, Shahrekord University, Shahrekord, 88186-34141, Iran
[b] Department of Civil Engineering, College of Engineering, Cihan University-Erbil, Erbil, Iraq
[c] Department of Petroleum Engineering, Al-Amarah University College, Maysan, Iraq
[d] Energy Department, Politecnico di Milano, Via Lambruschini 4, 20156, Milan, Italy

ARTICLE INFO

Keywords:
Insulation
Multi-objective-optimization
Heating and cooling setpoint temperature
Heating load
Cooling load
Thermal comfort

ABSTRACT

The uncontrollable rise in energy consumption become a most significant issue in recent decades. One of the largest consumers of energy resources across all industries is the residential building sector. Researchers have suggested several strategies to reduce energy loss, including enclosing insulation in wall structures because air conditioning systems account for the majority of energy use inside homes. The main goal of this article is to increase residents' thermal comfort (T_c) while reducing their heating load (H_L) and cooling load (C_L). Using the EnergyPlus program, the building model was simulated in sample cities with various climatic conditions. For optimization, the first seven design variables were determined in Jeplus software and then multi-objective optimization was performed by the Non-dominated Sorting Genetic Algorithm (NSGA-II) algorithm. As a result, T_c, HL, and CL values improved by 38–62, 61 to 100, and 17 to 39 percent, respectively.

Nomenclature

H_L	Heating Load
Tc	Thermal comfort
Cspt	Cooling set point temperature
I_t	Insulation type
I_{th}	Insulation thickness
Clo_w	Clothing insulation level winter
C_L	Cooling Load
Hspt	Heating set point temperature
MSA	Morris's sensitivity analysis
I_p	Insulation position
Clo_s	Clothing insulation level summer

* Corresponding author.
** Corresponding author.
E-mail addresses: mohamadbaghoolizadeh@gmail.com (M. Baghoolizadeh), asad.alizadeh2010@gmail.com (A. Alizadeh).

https://doi.org/10.1016/j.csite.2024.104491
Received 12 February 2024; Received in revised form 15 April 2024; Accepted 4 May 2024
Available online 6 May 2024

Table 1
An extensive analysis of earlier research.

Ref.	Insulation Type	Methods & Optimization	Year	Optimum insulation thickness	Sensitivity Analysis	Objectives	Station
Bojic et al. [10]	Polystyrene, Mineral wool	HTB2	2000	Yes	No	Cooling Load	Hong Kong
Bolattürk [11]	Polystyrene	–	2007	Yes	No	Base Temperature, Cooling Load, Heating Load	Seven selected cites of Turkey
Actacir et al. [12]	Extruded Polystyren Foam	–	2009	Yes	No	Cooling Load	Adana
Karaguzel et al. [49]	Extruded polystyrene	Energy Plus, GenOpt	2013	Yes	No	LCC (Life Cycle Cost)	Chicago
Ozel [13]	Extruded Polystyrene, Expanded polystyrene	MATLAB	2013	Yes	No	Cooling Transmission Load, Cost, Time Lag, Incident Solar Radiation	Antalya
Basniassadi et al. [50]	Insulation (0.041 W/m.K)	Energy Plus, Genetic algorithm	2016	Yes	No	Total Cost	Six selected cites of Iran
Bellos et al. [51]	Polystyrene	TRNSYS, EQUEST	2016	Yes	No	Cooling Load, Heating Load,	Greece
Solgi et al. [52]	Insulation (0.04 W/m.K)	Energy Plus	2018	No	No	Cooling Load, Heating Load, SPP	Four selected cites of Iran
Mitsopoulos et al. [53]	Insulation (0.04 W/m.K)	TEE-KENAK	2018	Yes	No	Cooling Load, Heating Load, SPP, CO_2 Generation	Four selected cites of Greece
Markarian and Fazelpour [54]	XPS Extruded Polystyrene	Energy Plus, Genetic algorithm	2019	No	No	Energy Saving, SPP CO_2 -SO_2 Emission	Five selected cites of Iran
ÇAĞLAYAN et al. [55]	EPS	–	2019	Yes	No	Cooling Energy, Heating Energy, LCC, SPP	Turkey
Wang et al. [56]	Foam glass Mineral wool Expanded polystyrene Foamed polyurethane Foamed polyvinyl chloride Expanded polyethylene	–	2020	Yes	No	LCC (Life Cycle Cost), SPP	Five selected cites of China
Huang et al. [57]	XPS EPS Polyurethane Glass fiber Aerogel Blanket	–	2020	No	No	Cooling Load, Heating Load, CO_2 Generation	China
Kishore et al. [58]	Expanded polystyrene	–	2020	No	No	Heat Gain, Cooling Load, Heating Load, Temperature	Five selected cites of USA
Rosti et al. [59]	Expanded polystyrene	–	2020	Yes	No	life-cycle cost, Cooling Load, Heating Load	Eight selected cites of Iran
Aydin and Biyikoğlu [60]	XPS	–	2021	Yes	No	Insulation Cost, Annual Energy Cost, SPP	Turkey
Kallioğlu et al. [61]	XPS, EPS	–	2021	Yes	No	Cooling Load, Cost, SPP	Jaipur
Küçüktopcu and Cemek [62]	XPS, EPS, RW, GW, Polyurethane	Artificial neural network	2021	Yes	No	Annual total net savings, Reduction of carbon dioxide emissions	Ankara, Madrid, Beijing, Tokyo, Prague, Washington
Dylewski and Adamczyk [63]	Mineral wool Polyurethane EPS Polyurethane XPS	–	2021	Yes	No	NPV, NPVE, MK	Four selected cites of Poland
Akan [64]	Rock wool, XPS, EPS, PUR	MATLAB	2021	Yes	No	Cooling Load, Heating Load, Annual net savings, SPP	Turkey

(continued on next page)

Table 1 (*continued*)

Ref.	Insulation Type	Methods & Optimization	Year	Optimum insulation thickness	Sensitivity Analysis	Objectives	Station
Baghoolizadeh et al. [23]	XPS Mineral wool Polyurethane Fiberglass Cellulose	Energy Plus, RSM	2021	Yes	Yes	Annual Electricity Consumption Cost, Total Load (Sum Cooling Load & Heating Load), SPP, Incident Solar Radiation, Thermal Comfort (PPD-PMV)	Five selected cites of Iran
Bagheri-Esfeh and Dehghan [65]	XPS, Fiberglass, Polyurethane	Energy Plus, RSM, GMDH neural network, NSGA-II	2022	Yes	No	SPP, PPD	Five Selected Cites of Iran
Baghoolizadeh et al. [24]	XPS, Mineral wool, Polyurethane	Energy Plus, RSM, GMDH neural network, NSGA-II	2023	Yes	No	Annual cost electricity consumption building, Cost of insulation & PCMs	Eight selected cites of Iran
Present study	XPS, Polyurethane, fiberglass, Mineral wool, Cellulose, Aerogel	Energy Plus, JePlus, Jeplus + EA NSGA-II	2024	Yes	Yes	Heating load (H_L), Cooling load (C_L), PPD	Four selected cites of Iran

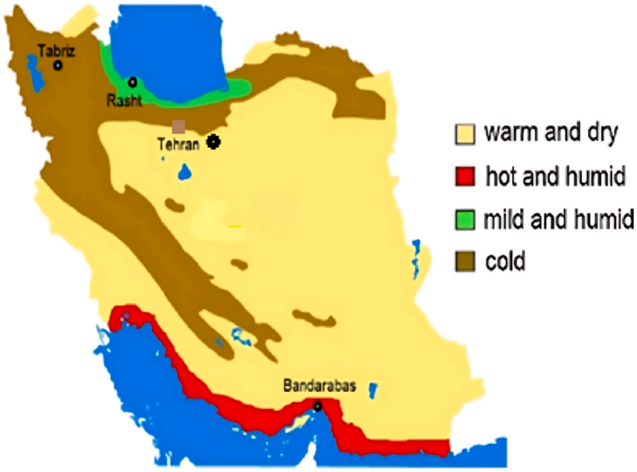

Fig. 1. Climate map of Iran [75].

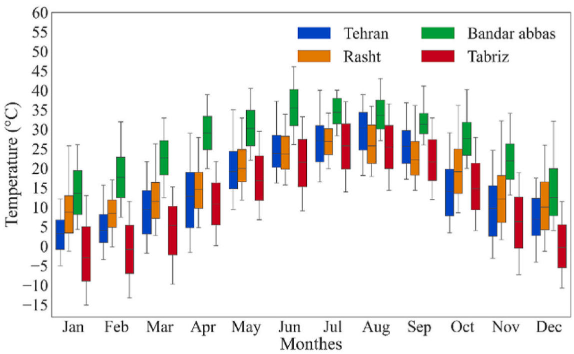

Fig. 2. Temperature variations for four cites [76,77].

1. Introduction

The importance of energy is becoming clearer in light of the quick industrial and economic advancements in contemporary societies [1]. One significant crisis of the 20th century can be categorized as excessive energy consumption. In many different industrial, commercial, and residential sectors, there is a sizable amount of energy dissipation, and in nations with extreme climatic conditions, this intensity increases [2]. According to statistics, households use between 30 and 40 percent of the energy consumed in urban areas [3,4], and more recent data indicates that households account for about 40 % of all primary energy consumption [5]. Cities with lower industrial activity and extreme climates can increase this amount of energy use to about 70 % [6]. Once it was discovered that

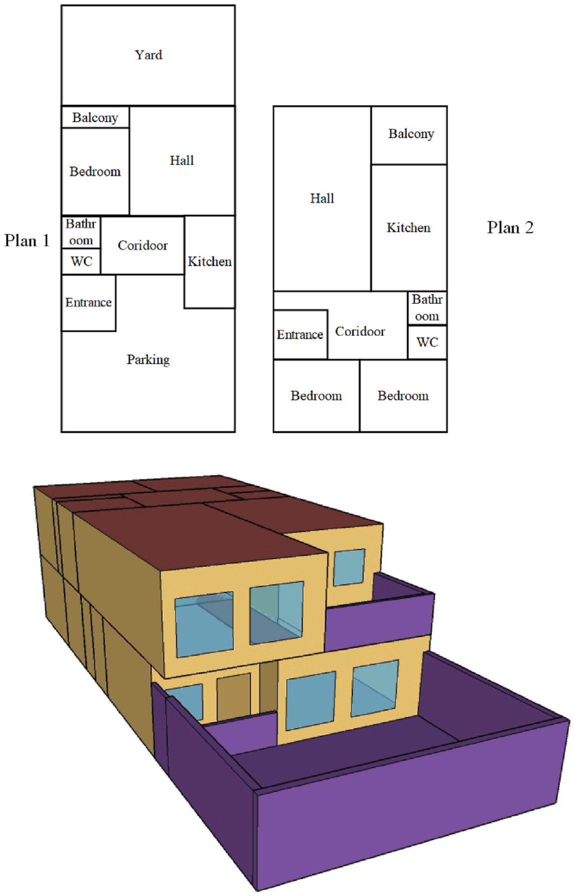

Fig. 3. The building that EnergyPlus used to simulate it for this study.

Table 2
Physical characteristics of building spaces.

Floor	Spaces	Floor area (m^2)
One	Bedroom	14.27
	Parking	38
	Kitchen	10
	Bathroom	2.66
	Toilet	2.18
	Living room	27.65
	Staircase and Entrance	6.5
	Bedroom 1	13.43
	Bedroom 2	13.29
Two	Kitchen	20.78
	Bathroom	2.81
	Toilet	2.81
	Living room	38.63
	Staircase and Entrance	5.89

energy loss from buildings is a contributing cause of greenhouse gas emissions, this issue became more serious. In recent years, global CO_2 emission has skyrocketed to approximately 10^{13} kg CO_2/yr, around one-fourth of which is attributed to residential buildings [5,7]. According to numerous researchers, the main cause of this issue is HVAC systems, which are used to heat and cool buildings [6,8–10]. According to Bolattürk [11], the increase in energy consumption is a result of urbanization, a rise in population in cities, and other factors. Because of this, researchers have looked into materials like insulators and phase change materials as they would be able to decrease energy loss. One of the intriguing topics for researchers to investigate the quantitative and qualitative energy savings of a building has been the impact of adding insulators to the building envelope.

For an area with a high cooling demand, Actacir et al. [12] tested 3 types of insulation with varying thicknesses, and, they were able to reduce the cooling load in addition to the cost of air conditioning by 33 %. Bojic et al. [10] investigated the thickness and

Table 3
Materials and their physical characteristics [78].

Material	Density (kg/m^3)	Roughness	Specific heat (J/kg. K)	Thickness (m)	Conductivity (W/m. K)
Marble	2700	Rough	790	0.02	3.5
Cement board	1800	Medium Rough	880	0.025	1.3
XPS insulation	28	Rough	1210	can be seen in the optimization section	0.041
Block	1800	Rough	790	0.105	1.17
Polyurethane Insulation	24	Rough	1590	can be seen in the optimization section	0.0245
Gypsum Board	1300	Medium Smooth	1090	0.03	0.57
Concrete	1300	Very Rough	880	0.1	0.44
Fiberglass	64	Rough	960	can be seen in the optimization section	0.036
Brick facade	2000	Medium Rough	790	0.04	1.33
Cellulose	120	Rough	1400	can be seen in the optimization section	0.045
Waterproofing membrane	2000	Very Rough	1120	0.02	1.15
Mineral wool	150	Rough	1030	can be seen in the optimization section	0.033
Aerogel	60	Rough	750	can be seen in the optimization section	0.013
Concrete block	2100	Medium Rough	920	0.2	1.33

Table 4
Materials used in the construction of various construction layers.

Construction	Layer 1	Layer 2	Layer 3	Layer 4	Layer 5
Roof (outside)	Gypsum Board	Concrete block	Concrete	Insulation	Water Proofing Membrane
Exterior wall (outside)	Gypsum Board	Block	Cement board	Insulation	Brick facade
Roof (inside)	Gypsum Board	Concrete block	Insulation	Concrete	Water Proofing Membrane
Exterior wall (inside)	Gypsum Board	Insulation	Block	Cement board	Brick facade
Roof (Both sides)	Gypsum Board	Insulation	Concrete block	Concrete	Water Proofing Membrane
Exterior wall (Both sides)	Gypsum Board	Block	Insulation	Cement board	Brick facade
Ceiling/Floor	Gypsum Board	Concrete block	Cement board	Marble	–

Table 5
Optical properties of glass material for different geographical windows [79].

Geographical location of the window	Properties	Unit	value
South/North	Total heat transfer coefficient (U (	$\frac{W}{m^2K}$	3.1
	Solar heat gain coefficient	–	0. 5
	Visible transmittance	–	0.55

Table 6
Luxury values of electricity usage of several building spaces [80].

Zone	Lux
Bedroom1	100
Bedroom2	100
Bedroom3	100
Kitchen	200
Living room	200
Bathroom	100
Toilet	100
Entrance	150
Parking	150

placement of the wall insulation with variable concrete thickness and optimized the cooling demand and cooling load by 7 % for a house model located in Hong Kong. Using the Degree Law method, Bolattürk et al. [11] were able to calculate the energy-saving [\$/m^2], determine the proper payback period for both cooling and heating load, and optimize insulation, They assumed a restriction of transmission load which can affect both cooling and heating load. In a hot climate city where cooling was required, Ozel [13] thought about the effects of changes in insulator thickness. He discovered that by determining the ideal insulator thickness, the northern wall has the lowest cooling load and the western and eastern walls have the highest. Additionally, a 3 cm thick insulator was used to optimally reduce the cooling load by about 66 %. Yu et al. [14] was examined how surface color and wall orientation affected the ideal thickness of various insulation materials in four typical Chinese cities. Even though wall orientation was listed as a significant contributing parameter, there was no discernible pattern in the impact of surface color. It was thought that expanded polystyrene could be the most practical insulation material. Nematchoua et al. [15] investigated two common wall structure types with four cardinal directions. The best case was described as a south-facing wall with 9 cm of insulation, 79.8 % energy savings, and a 4.73-year payback period. Using the P1–P2 economic method for some constructions in Cameroon, Cyrille Vincelas and Ghislain [16] evaluated

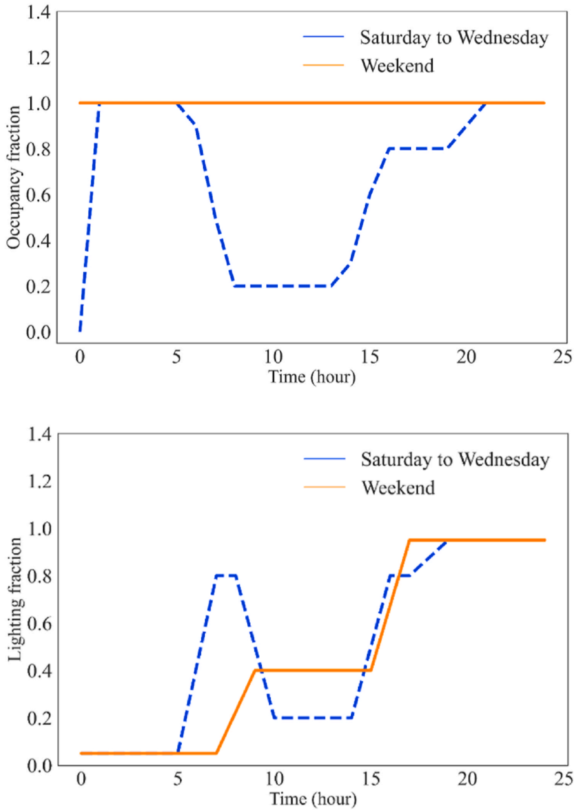

Fig. 4. Building lighting quantity and occupancy hours [80].

Table 7
Compares the numerical data from the current study with Muruganantham [82] experimental observations.

Month	Energy usage (kWh)		Error(%)
	EnergyPlus	Experimental	
June	288	273	5.5
July	319	319	0
August	308	293	5.1

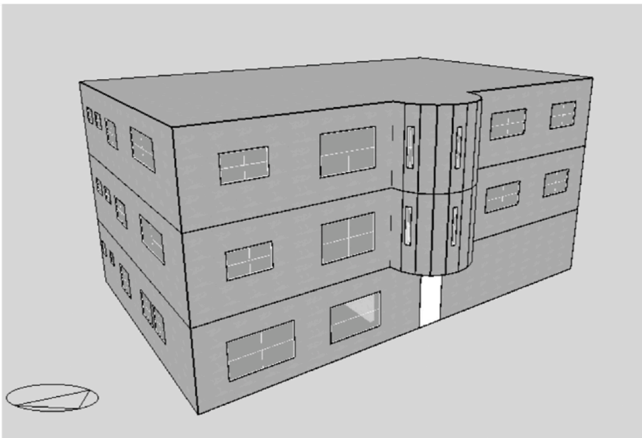

Fig. 5. The building is simulated in the software.

Table 8
Comparison of building energy consumption in two experimental [84] and numerical modes.

	Energy consumption by experimental (kWh)	Energy consumption by EnergyPlus (kWh)	Error percentage (%)
Cooling	23649	23350.18	1.27
Heating	77784	74415.31	4.33
Total	101433	97765.49	3.62

Table 9
Design variables.

Design variable	Unit	Type	Range
Cooling Setpoint (Cspt)	°C	Continuous	(23,28.5)
Clothing insulation level for summer (Clo_s)	Clo	Continuous	(0,2)
Insulation type (I_t)	–	Discrete	XPS, Polyurethane, fiberglass, Mineral wool, Cellulose, Aerogel
Insulation thickness (I_{th})	*Cm*	Continuous	(0,10)
Insulation position (I_p)	–	Discrete	Outside, Inside, Middle
Clothing insulation level for winter (Clo_w)	Clo	Continuous	(0,2)
Heating Setpoint (Hspt)	°C	Continuous	(17, 22.5)

Table 10
Sensitivity analysis of design variables in relation to objection functions.

Design variables	Objective functions					
	H_L		C_L		T_c	
	μ	σ	μ	σ	μ	σ
Cspt	246.5	194.4	11630	1381	12.12	10.78
Clo_s	0	0	0	0	36.7	38.14
I_t	1903	1900	3468	4342	0.9614	0.9004
I_{th}	3211	2513	5840	5794	2.282	3.115
I_p	131.9	98.45	391.6	143.9	0.2236	0.1435
Clo_w	0	0	0	0	54.57	37.71
Hspt	9877	1389	329.3	229.5	11.29	9.225

Table 11
The preliminary values of the objective functions before optimization.

Cites	T_c (%)	CL (Kwh)	HL (Kwh)
Tehran	22.688	11909.24	19088.2
Tabriz	30.877	4983.91	36638.28
Rasht	22.28	8602.68	16878.24
Bandar Abbas	27.609	49304.91	182.23

seven insulation materials used in five common wall structures. The ideal thickness, energy savings, and payback periods varied depending on the type of wall, falling in a range of 8–10 cm, 44–150 ($/m2), and 0.91–2.21 years, respectively. The sundry earth block (SEB) with 9 cm extruded polystyrene was also the best wall option. Liu et al. [17] conducted a different study in China that assessed the ideal thickness taking moisture transfer through the wall into account. They showed that underestimating insulation thickness and energy savings while overestimating the payback period resulted from neglecting moisture transfer. In eight representative Palestinian governorates, Alsayed and Tayeh [18] examined the ideal thickness for various common exterior insulation types and wall constructions. For every case, the measurement ranged between 0.4 and 9 cm. Shekarchian et al. [19] determined the optimal thickness of a few common insulators in Malaysia using the most desirable insulation, fiberglass-polyurethane, which has a 2.2 cm thickness and can reduce costs by 1.8 dollars per square meter. In Tunisia, Daouas et al. [20] used an analytical approach to resolve the 1D heat transfer equation for an exterior wall during the cooling. To find out the optimal insulation thickness by life-cycle cost analysis, two commonly used wall structures and 2 types of insulation were chosen. The most successful application achieved a 58 percent energy saving and a payback period of 3 years with a sandwich wall made of stone and brick and expanded polystyrene measuring 5.7 cm. D'Agostino et al. [21] measured the optimal thickness of insulation for cities in the south and north of Italy, specifically Palermo and Milan, and compared them to Cairo, Egypt. Based on their research, the best thicknesses for Milan and Palermo were 8–10 cm and 2–4 cm, respectively. Unexpectedly, insulation never benefited Cairo. In Greece, cardinal orientations were taken into account by Tzoulis and Kontoleon [21] to suggest the ideal insulation thicknesses. The findings demonstrated that depending on wall orientations, the ideal extruded polystyrene thickness was variable between 7.5 cm and 10 cm. For two aerated brick and concrete walls in Tehran, Iran, Ramin et al. [22] optimized two types of insulation (extruded and expanded polystyrene). According to the results, the ideal thickness was variable between 1 cm and 7 cm, the calculated energy savings ranged from 31 to 82 percent, and the payback pe-

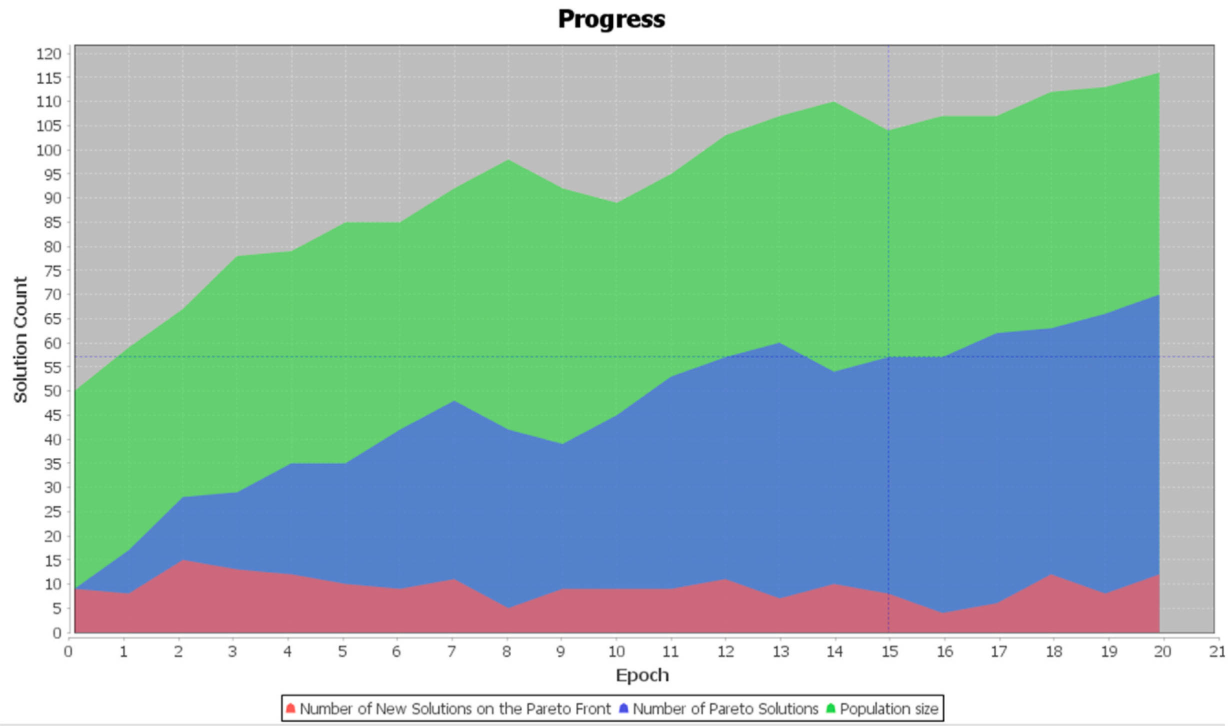

Fig. 6. Convergence diagram of the genetic algorithm for the problem of the present study.

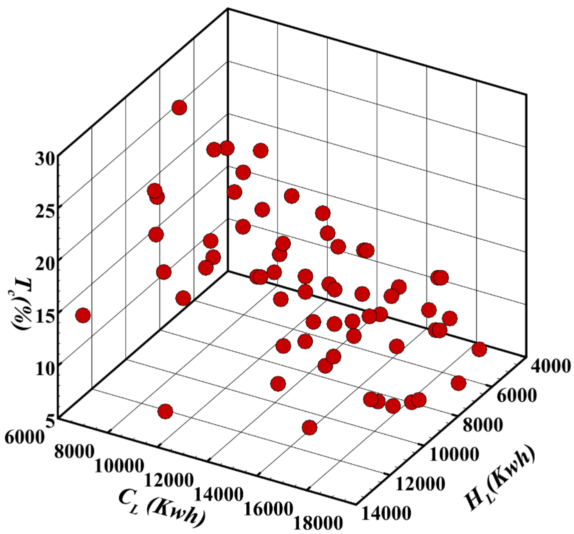

Fig. 7. Tehran's top points from the Pareto front.

riod was in the range of 4–18 years. For the four primary orientations connected to vertical and horizontal walls, these values were calculated about wall and insulation types. Baghoolizadeh et al. [23] used 5 types of insulation in the north, south, east, and west walls. They use the level response method to optimize the amount of load and cost of the building. They were able to improve the thermal load and cost of the entire building in different weather conditions by 2 %–16 %, and dramatically improve occupant's heating comfort and the static payback period. In another study, Baghoolizadeh et al. [24] studied phase change materials in addition to insulation for different climates in Iran. Using an artificial neural network, they extracted the relationship between decision-maker variables and objective functions. Afterward, using the Genetic algorithm (GA), they optimized the annual electricity consumption cost along with the insulation and phase change materials costs for their building model. They found that the use of insulation and PCM with optimal properties can minimize the objective functions in the range of 12–18 % in cold, temperate, and semi-arid cities, but PCM and insulation are not recommended for hot and humid cities.

Table 12
The specifications of Tehran's Pareto front's ideal points.

Coefficient (a_1)	Cspt (°C)	Clo_s (Clo)	I_t	I_{th} (cm)	I_p	Clo_w (Clo)	Hspt (°C)	PPD (%)	H_L (kWh)	C_L (kWh)
0	28.5	1.6	Aerogel	0.09	Outside	1.15	19	25.532	7366.8	6350.36
0.1	28.5	1.25	Aerogel	0.095	Outside	1.45	20	19.602	8794.38	6334.58
0.2	28.5	0.75	Aerogel	0.075	Middle	1.4	17	18.29	4862.18	6547.67
0.3	28.5	0.8	Aerogel	0.075	Outside	1.3	20	15.764	8948.85	6496.92
0.4	28	0.5	Aerogel	0.085	Inside	1.2	20.5	13.761	9676.81	7302.73
0.5	26.5	0.8	Aerogel	0.08	Outside	1.45	18	12	6123.33	9534.29
0.6	26	0.7	Aerogel	0.045	Middle	1.45	18.5	11.024	7139.86	11263.5
0.7	25	0.95	Polyurethane	0.075	Inside	1.6	18	9.508	6631.42	13494.5
0.8	23.5	1.2	Aerogel	0.065	Middle	1.7	17	8.482	5012.16	15615.9
0.9	23.5	1.15	Polyurethane	0.06	Middle	1.5	19.5	7.467	9066.83	17147.7
1	24	1	Aerogel	0.085	Middle	1.35	21.5	6.619	11628.6	14501.8

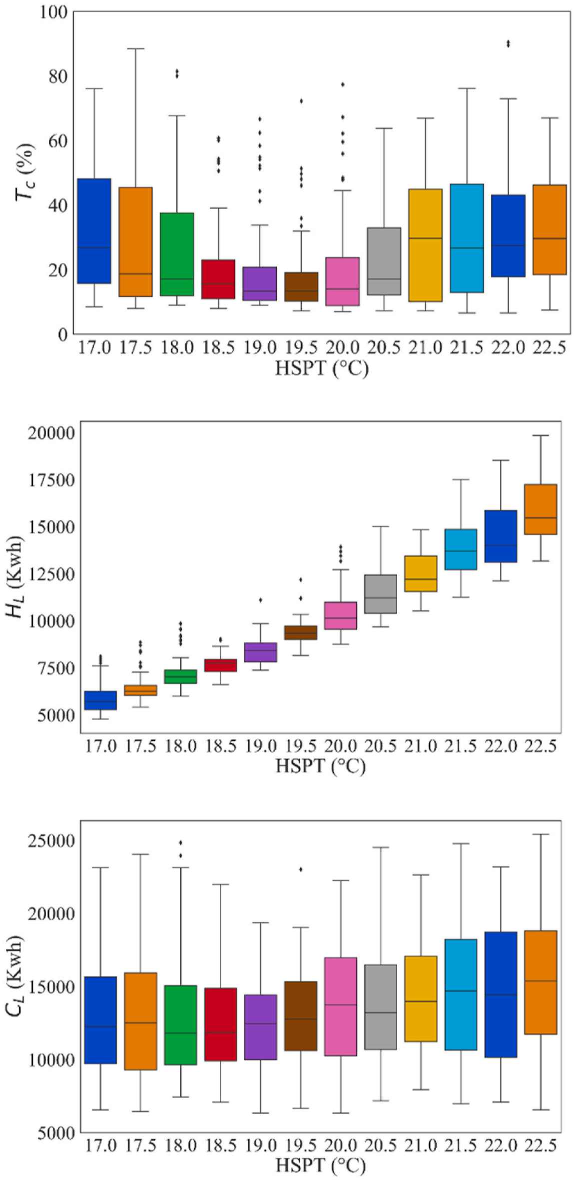

Fig. 8. HSPT changes on objective functions in Tehran city.

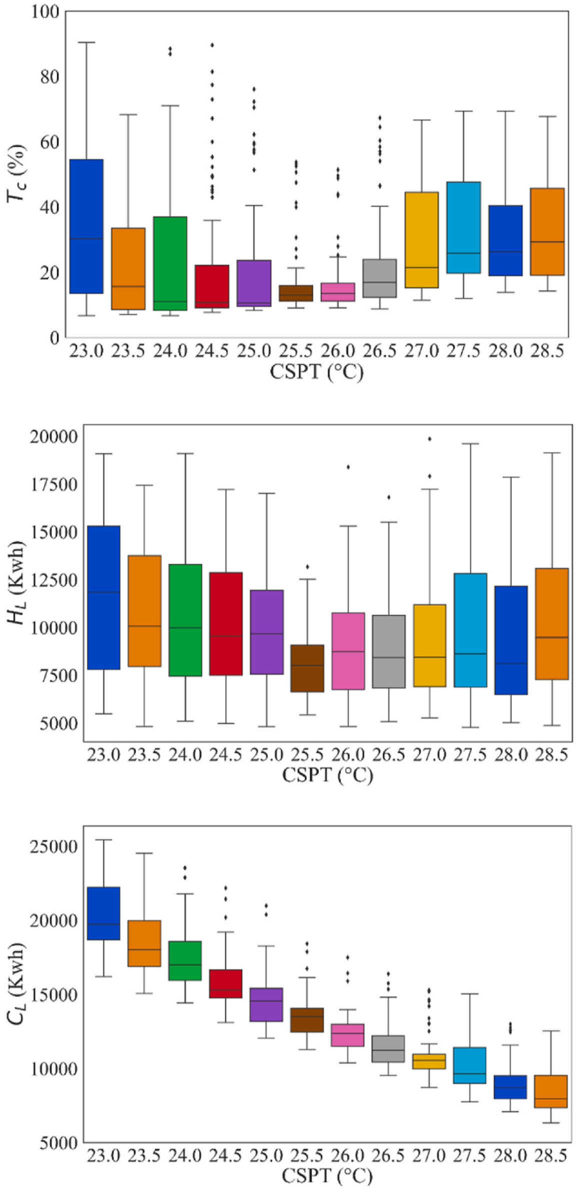

Fig. 9. CSPT changes on objective functions in Tehran city.

It is clear that finding the ideal state, such as the ideal cooling load, is the typical procedure in the studies mentioned above. It is significant to note that finding the ideal situation calls for optimization-related techniques and algorithms. Engineering problems are frequently solved using optimization methods. The GA was created with the NSGA initial version, and the NSGA-II, the updated version, was published in 2002 [25]. This algorithm has the benefit of an unconstrained variable selection that accepts both discrete and continuous variables. This algorithm has been employed by a variety of engineering disciplines. Also, we can mention that this algorithm and other methods in ANN have been employed by a variety of researchers [24,26–42]. To be optimized and used, this algorithm requires numerical coding in several software components. The easiest option is to use JEPLUS + EA software, which does not require programming and does not have to deal with the complexity of this algorithm. It is very challenging for scientists to choose the best objective function because the majority of optimization problems have multiple objective functions [23], which are also in conflict with one another and grow larger as one shrinks. The Pareto front, a set of optimal points that the user is shown by the NSGA II algorithm, enables the user to choose the optimal point that most closely matches his aims [43,44]. Combining this program with Energy Plus software makes optimization tasks simple to complete. Naderi et al. [45] analyzed the development of intelligent Venetian blinds. They could minimize sunlight glare, annual electricity consumption, and resident dissatisfaction in six Iranian cities by applying a variety of shading management strategies to optimize the shading. Delgarm et al. [46] investigated the effects of various architectural elements, such as the direction of the building, the size of the windows, and the need for shading to optimize the building's energy use for each of Iran's four major climate zones—cold, mild, hot-dry, and hot-humid. Using the GA, they increased the annual

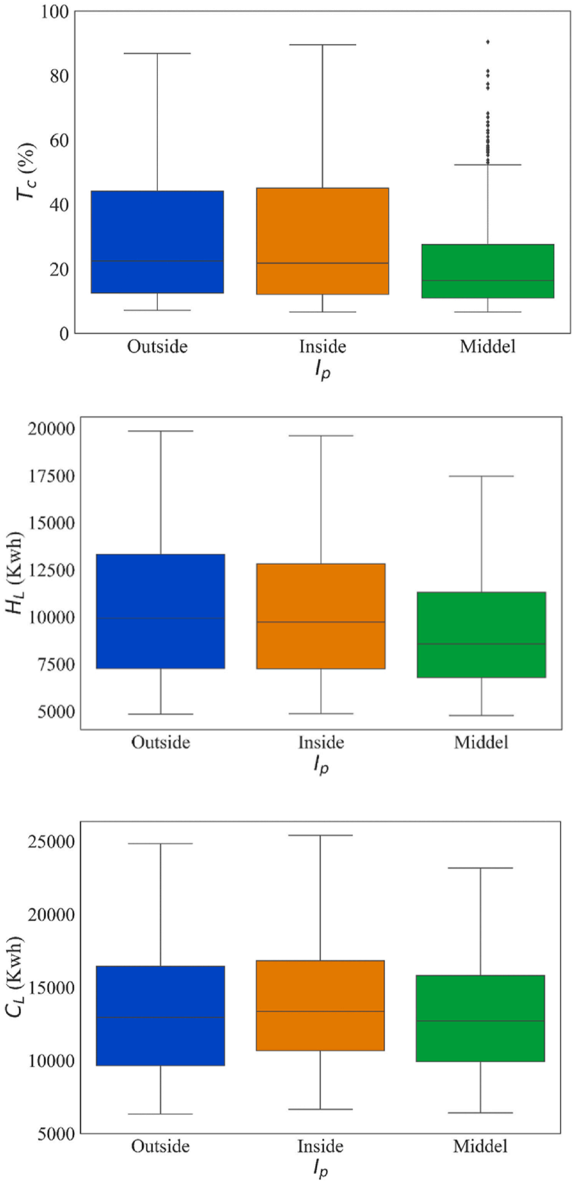

Fig. 10. I_p changes on objective functions in Tehran city.

electricity demand by 1–4.8 percent while decreasing the annual energy consumption for cooling by 55.8–76.4 percent. This led to a 23.8 to 42.2 percent reduction in annual energy use. To improve the horizontal shading parameters on a building's southern façade in a semi-arid climate in Morocco, Sghiouri et al. [47] looked into potential methods. They reduced the cooling load by more than 4 % yearly. Bingham et al. [48] developed a solar system for Russia that is grid-connected and battery-powered. Their relative reductions in energy use, carbon emissions, and NPV life cycle were from 28 to 42 %, 25 %–30 %, and 90–100 %.

For a better literature review, several studies have been reviewed in Table 1. According to Table 1, the gap between the present research and other studies can be expressed as follows.

- In many studies, the main goal has been to investigate the cooling or heating load, but in addition to these two cases, it is important to establish thermal comfort for the residents, and these three cases are investigated in this study. This is done by a multi-objective optimization with the NSGA algorithm.
- In most studies, one or two types of insulation have been used, but in this study, 6 types of insulation common in the Iranian market have been used.
- The place of insulation is one of the things that has a direct effect on heat loss, which has been less investigated in previous studies. The level of suitable clothing of the residents of the building can affect the thermal comfort of the residents, which is investigated in this study.

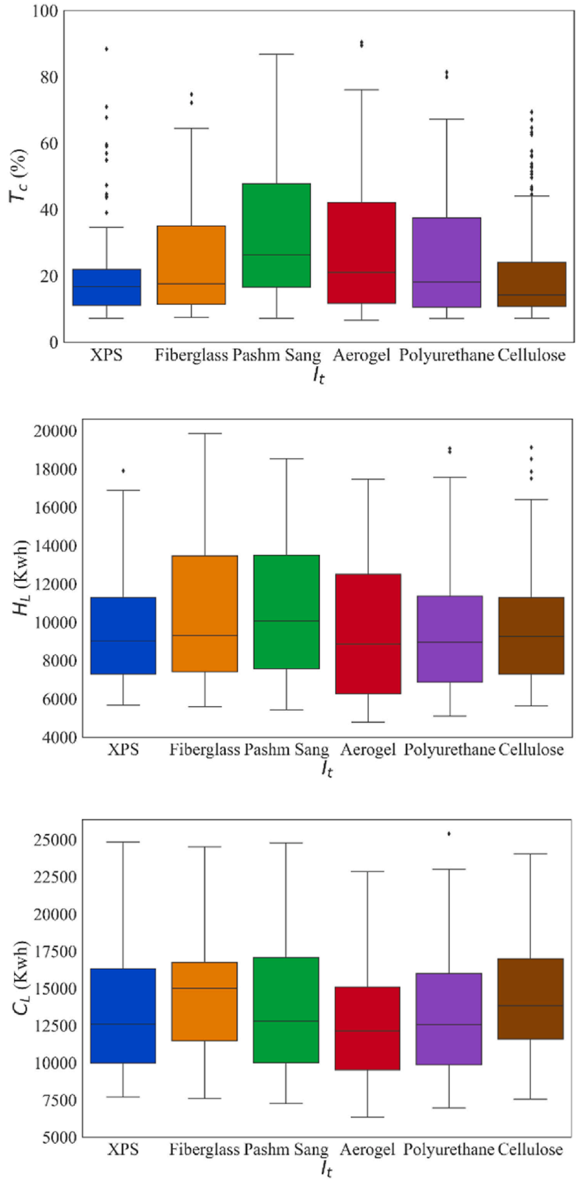

Fig. 11. I_t changes objective functions in Tehran city.

- The temperature of the cooling and heating thermostat directly affects the cooling and heating loads, which is investigated in this study.

Most researchers focus on discovering the optimal insulation for a particular climate, while in the present research, four targeted cities have varying climatic features. Energy simulation is done by EnergyPlus software. Jeplus software has been used to introduce and design the variables. The design variables in this study are Heating set point temperature (Hspt (, Cooling set point temperature (Cspt (, Insulation position (I_p), Insulation type (I_t), Insulation thickness (I_{th}), Clothing insulation level summer (Clo_s) and Clothing insulation level Winter Clo_W. The goal of the present research is to improve T_c and reduce the H_L and C_L of the building. For this purpose, the NSGA-II algorithm is used for multi-objective optimization. After that, the optimal points, known as the Pareto front, are provided to the user to choose the best point among the points. Finally, the improved values of the objective functions are examined.

2. Numerical modeling

Utilizing a toolbox with an order of accuracy is desirable due to the experimental constraints and large volume of calculations. One case that has seen rapid advancements in recent years is the simulation of building performance [66]. To fulfill the goals of the current study, EnergyPlus one of the commercial software programs that is most applicable to the ventilation industries is integrated here. The use of Conduction Transfer Functions is the foundation for the energy-based computations in EnergyPlus, claims Under-

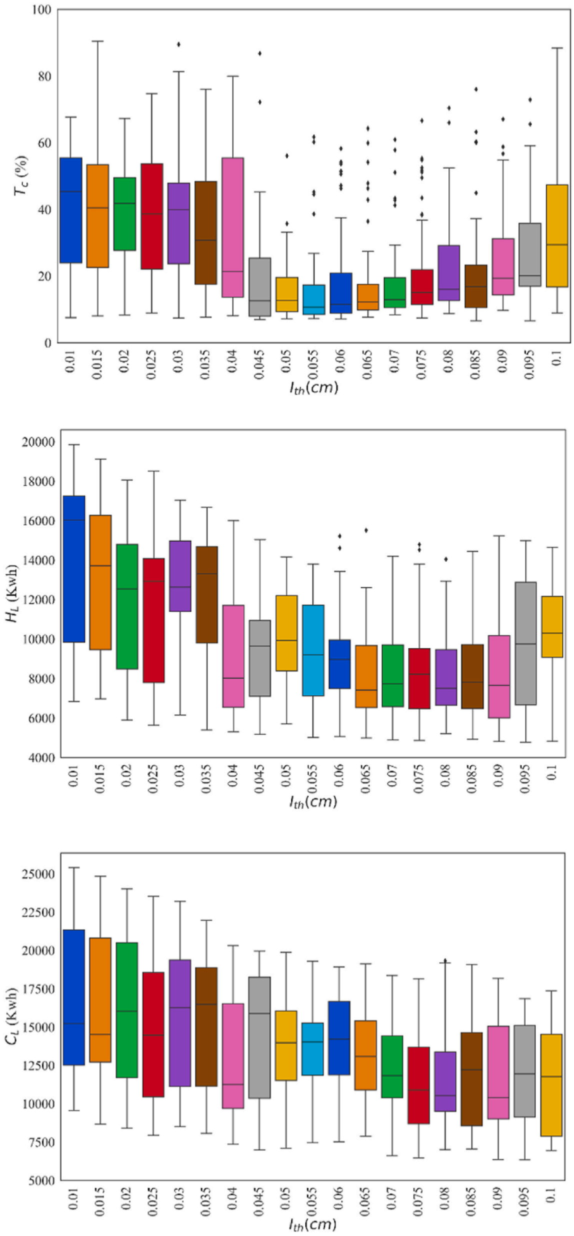

Fig. 12. I_{th} changes in objective functions in Tehran city.

wood [67]. This program has been employed by researchers in a variety of energy usages, including energy-saving prediction [68,69], heat transfer modeling [70,71], solar energy harvesting modeling [27,28,72], and prediction of room temperature [73,74]. It is necessary to account for a standard geometry to construct the objective functions in EnergyPlus before beginning the numerical computations. After introducing the EnergyPlus software, it must take into account several settings, including climate, building and envelope, building internal gain, HVAC system, and validation.

2.1. Climate

Iran is located in an area with dry weather. From the northern regions of Africa and the Middle East to the Iranian Plateau, this type of climate is extended. However, Iran is divided into four distinct climate zones: dry and warm, mild and humid, hot and humid, and cold zones [75]. As seen in Fig. 1, there are four cities were chosen for this study based on these climates. According to Fig. 1, the city of Tehran represents the warm and dry climate, the city of Bandar Abbas represents the hot and humid climate, the city of Rasht represents the mild and humid climate, and the city of Tabriz represents the cold climate.

One of the variables that need to be entered into the EnergyPlus software is the yearly variation in city temperatures. Fig. 2 illustrates how the four cities' temperatures changed for an entire year. According to Fig. 2, the hottest city is Bandar Abbas, and the oppo-

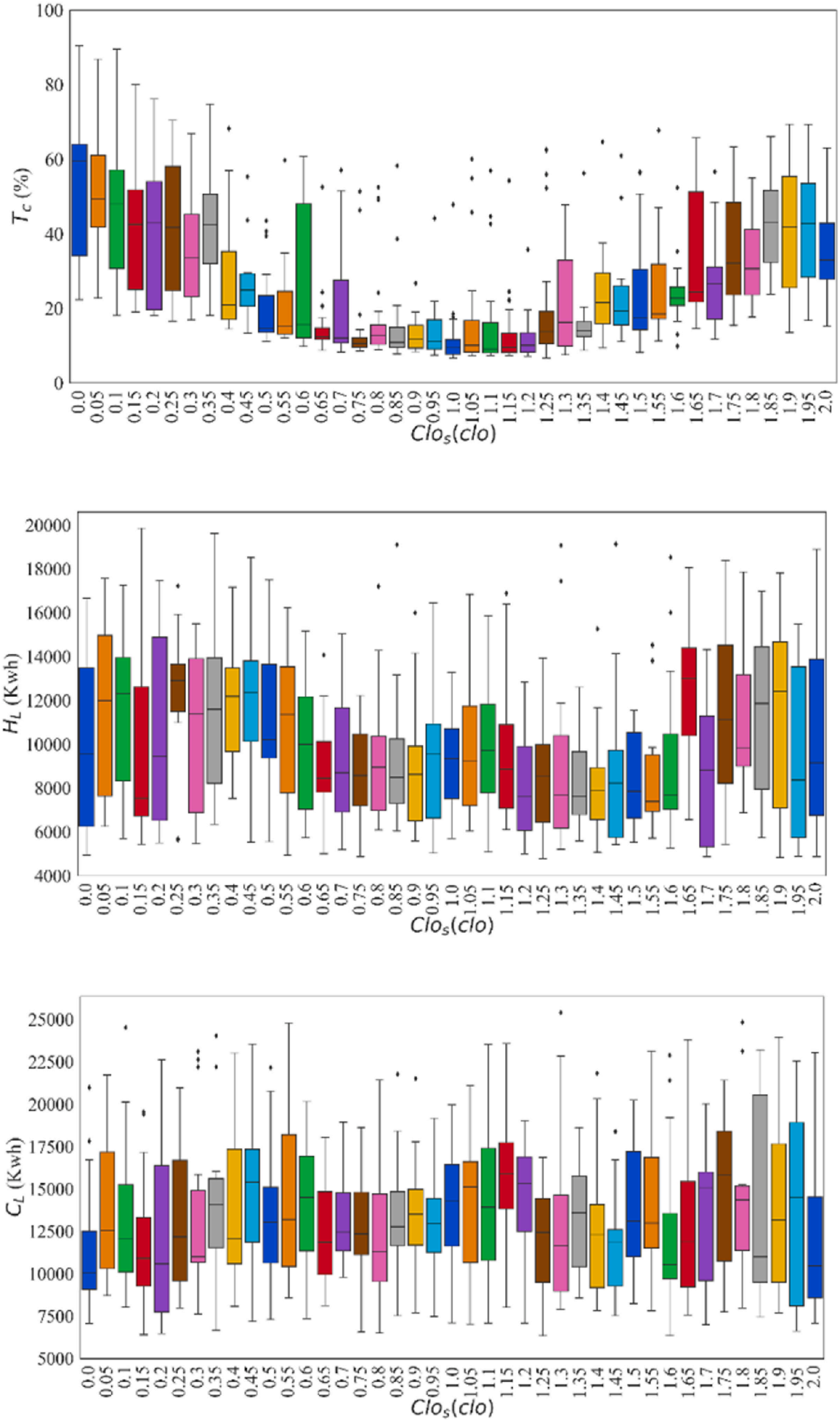

Fig. 13. Clo_s changes on objective functions in Tehran city.

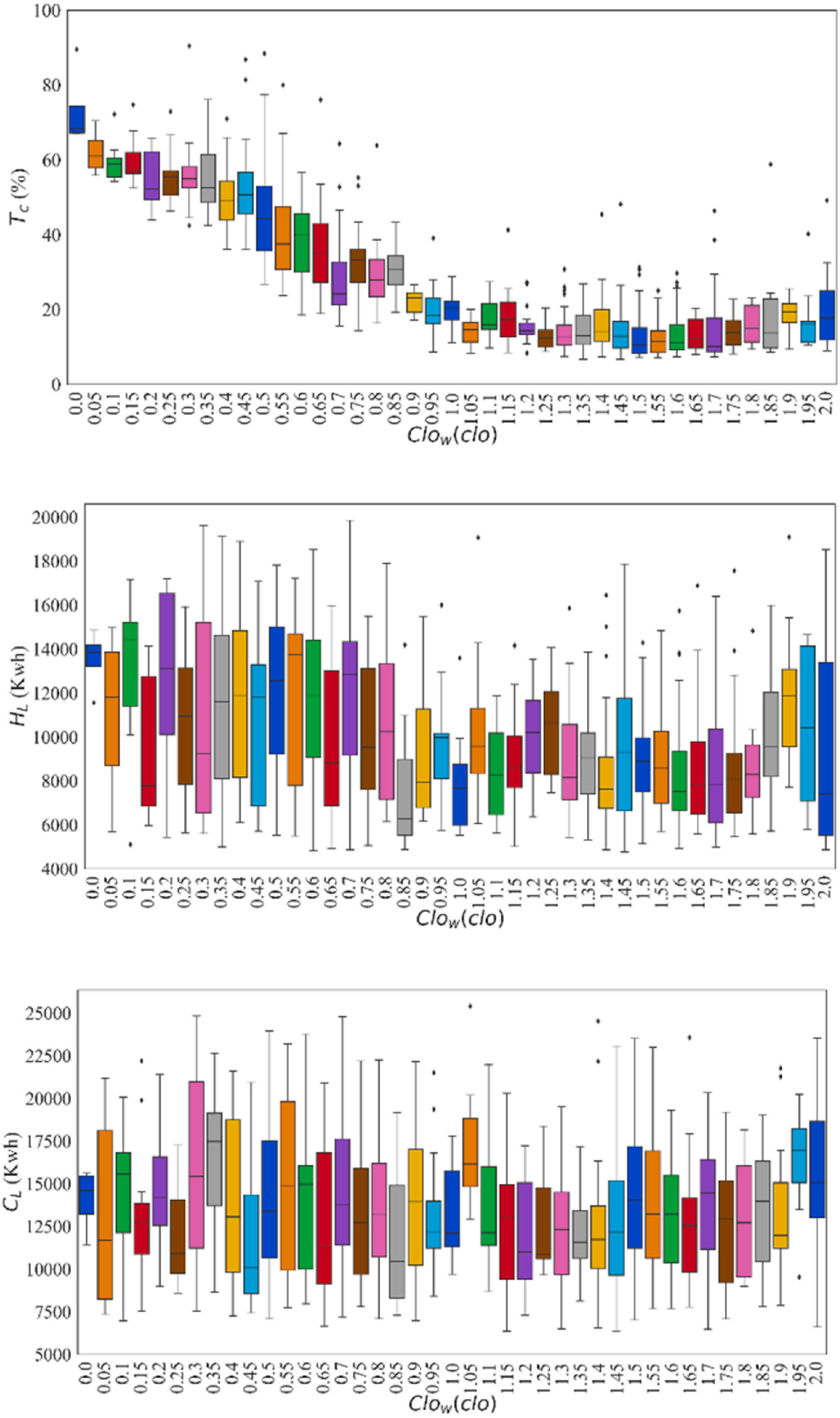

Fig. 14. Clo_w changes on objective functions in Tehran city.

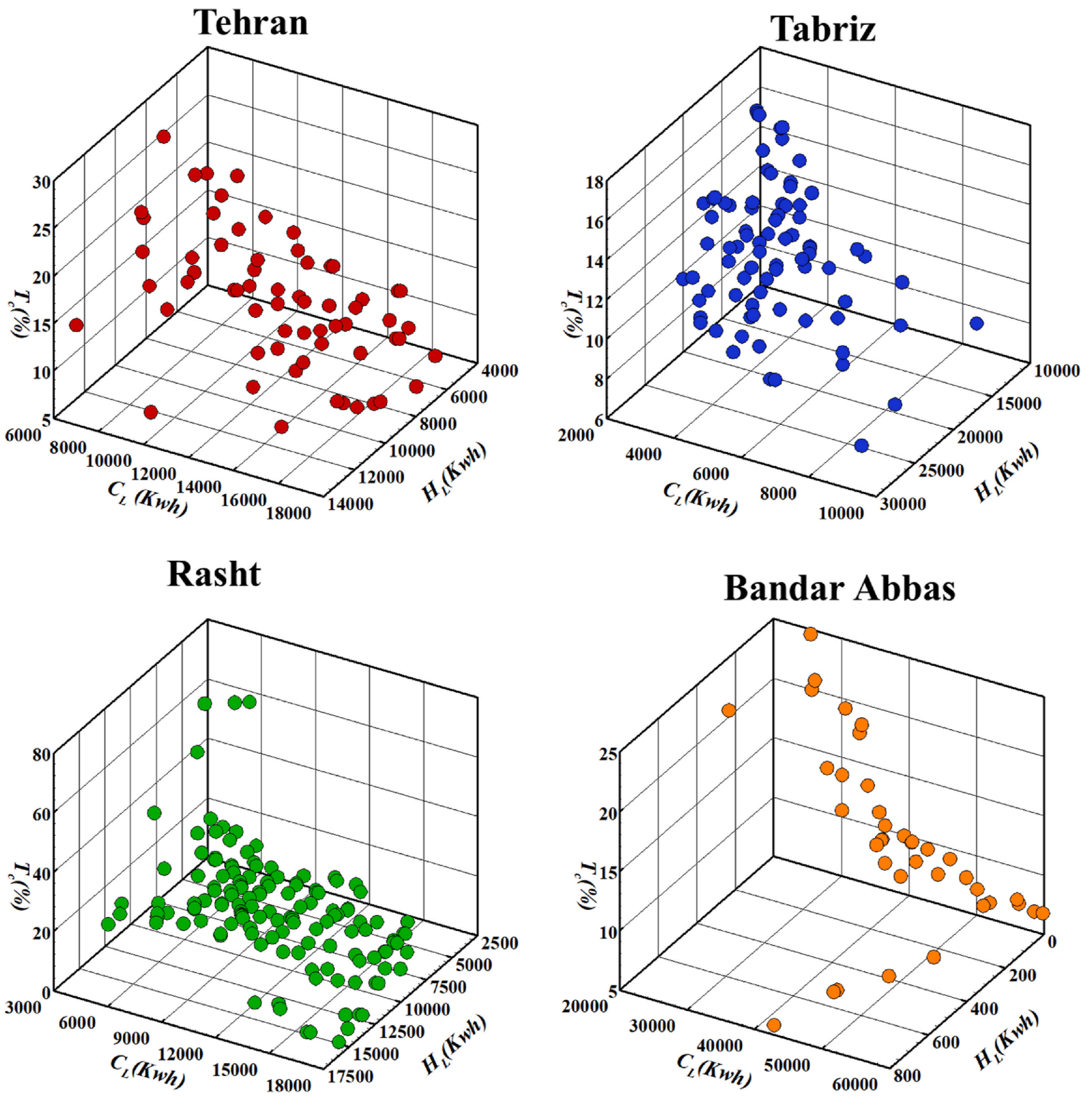

Fig. 15. Optimal Pareto front values for the studied cities.

Table 13
Characteristics of optimal Pareto front values for the studied cities.

Cites	Cspt (°C)	Clo_s (Clo)	I_t	I_{th} (cm)	I_p	Clo_w (Clo)	Hspt (°C)	PPD (%)	H_L (kWh)	C_L (kWh)
Tehran	26.5	0.8	Aerogel	0.08	Outside	1.45	18	12	6123.33	9534.29
Tabriz	27	1.15	Aerogel	0.09	Outside	1.9	18	12.368	14370.9	3644.11
Rasht	26.5	0.9	Aerogel	0.08	Inside	1.5	18	13.74	5227.3	7134.3
Bandar Abbas	27.5	0.2	Aerogel	0.095	Outside	0.6	18	10.56	0.84	30131

site is the coldest city, Tabriz. The city of Rasht has a moderate and humid climate, which has caused it to have pleasant weather in most months of the year. Also, Tehran has relatively cold winters and hot summers.

2.2. Building and envelope

The building under investigation in this study is typical in Iran. There are two floors in this building. A residential unit is located on the upper floor of the parking lot, as well as on the lower floor and next to the parking lot. The west side of this building borders another building. A bedroom, a living room, a bathroom with a toilet, and a kitchen are all on the first floor. The second floor is identical

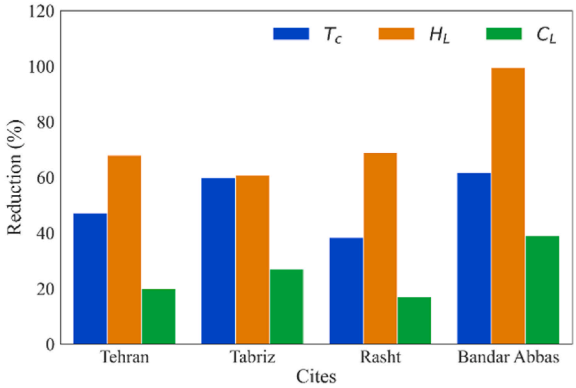

Fig. 16. Improved values of Tc, HL, and CL for the studied cities.

to the first floor except for having an additional bedroom. Fig. 3 and Table 2 display the building's shape, its features, and the size of the spaces.

The kind and density of the materials positioned in the walls are chosen to connect the building model with the context of Iranian architecture. According to Iran's national building laws and regulations, which are covered in Tables 3 and 4, the materials implemented for the current geometry in addition to their physical characteristics are taken into consideration. Three kinds of external walls, floors, and roofs are all included in the structure of various walls (but only to check where insulations should be placed best; see the section on optimization). Table 4 explains the materials used in the construction of various construction layers. Table 5 discusses specifics regarding the glass utilized in the structure.

2.3. Internal load and air conditioning system

Following Article 13 of Iran's building laws and regulations [80], four people are living inside the building on every floor. Moreover, Fluorescent lighting is considered for interior lighting. According to topic 19 of Iran's national building laws and regulations, no specific schedule has been provided for electrical equipment in the residential sector, but an average value of 4 W per square meter is considered for 24 h a day. In different areas of the building, the luxury lamp consumption is shown in Table 6. Also, the schedule of the presence of people and lighting is illustrated in Fig. 4. According to Fig. 4, the schedule of the whole week for the presence of people and lighting can be seen. According to this form, the days of the week are divided into two parts. The first part is from Saturday to Wednesday, when people leave their homes due to working hours, and the lighting and presence of people decreases. In the same way, the second part is related to holidays, Thursday and Friday, when people live inside the house, and the presence of people and lighting is more on the rest of the days.

For optimal design of an air conditioning system, it is necessary to calculate the building's cooling and heating load in the first step. For this purpose, Energy Plus software has provided a component called the ideal load air system, which helps the design engineer skip manual calculations and perform cooling and heating load calculations with this component. This system is a system with 100 % efficiency. This system can work with infinite or limited heating and cooling capacity. For both unlimited or limited capacity modes, the user can also specify on/off schedules for heating and cooling and outdoor air controls. There are also optional controls for dehumidification, dehumidification, economizer, and heat recovery. The system can be considered as an ideal unit that mixes the air in the exhaust conditions of the area with the specified amount. Adds or removes outside air and then heat and humidity at 100 % efficiency to produce supply airflow at specified conditions [81]. To control the temperature of the spaces, a thermostat must be specified for cooling and heating. According to topic 19 of the national building laws and regulations [78], the heating temperature is set at 20 °C, and the cooling temperature is set at 25 °C for cities with hot and humid weather and 28 °C for other cities.

The geometry is considered as a typical building, since most of the building constructed in Iran is very similar to the present study case and only there some small detail that are different from study case. With respect to climate situation a vast area of Iran is warm and dry. Hence, Architects apply customary materials for foundation and construction of building. It is worth mentioning that these materials are recommended by topic 19 of Iran's national construction laws and regulations. The number of people in buildings is different. The increase in number of residents in the building causes more metabolism and more activity in the space, and with increased activity and heat production, thermal comfort may be disturbed and cause heat production. But the rate of heat produced from the activity is very low and according to the Energy Plus commercial code, this value is below 10 % and can be ignored in many cases. The timetables used in present study is according to topic of 19 national laws and regulations of Iran. These timetables coincide with daily life of Iranian people.

2.4. Validation

To confirm the quality and validity of the data derived from the EnergyPlus software, a comparison between the numerical data from the current study and the experimental data from Muruganantham [82] has been made. Muruganantham's study [82] has been used for validation in several studies and is one of the most important studies for this work [23,24,83]. Within experimental research, Muruganantham [82] assessed the annual load for their building and the impact of thermal insulation and PCMs on the walls of a structure in Phoenix, USA. Muruganantham [82] compared its experimental outcomes to a simulation of the experiment's conditions using the EnergyPlus program. Because the current study's subject is comparable to that of Muruganantham [82], Compares Muruganantam et al.'s numerical and experimental results with the EnergyPlus calculations from the current study [82], as displayed in Table 7.

Table 7's findings show that there is a strong correlation between numerical and experimental data, and this supports the present study's calculations because the error range is within a 5 % margin.

For the second validation, in this study, from the study of Fathalian et al. [84] is used. In 2018, Fathalian et al. [84] conducted their studies on the three-story building of the Gas Department in Semnan. First, they simulated the office building inside the Design Builder software, then calculated the amount of heating and cooling energy of the building, and finally compared the data with the actual consumption values. In this research, they used one heater for the heating system and one heater for the cooling system. The simulated building can be seen in Fig. 5, as well as the comparison of the simulation results and the experimental study of Fathalian et al. [84] In Table 8.

The results show that the simulation data is close to the real data and its error is less than 5 %, which is acceptable for validation.

3. Preprocessing on data and optimization

In this part, design variables and objective functions are first introduced. Then Morris sensitivity analysis will be used to check the influence of input variables on the objective functions. Finally, a multi-objective optimization will be done and the best points will be selected by WSM.

3.1. Design variables and objective functions

EnergyPlus is one of the helpful tools for calculating energy-based parameters in buildings. Before it was released to the public, the US Department of Energy thoroughly tested each component of the software [73,85–87]. This software is used in numerous energy and construction-related studies [45,68,88]. Yi Zhang [89] introduced jEPlus software in 2012 to parameterize EnergyPlus. This program's design parameters can be specified in either numerical or categoric form, making it one of the most effective in the parameterization field when used with energy software [90,91]. Later, Zhang unveiled jEPlus + EA to enhance the software's capabilities, which included the ability to perform optimization (NSGAII) [45,46,92], sensitivity analysis [93–95], and a variety of random sampling methods [92,95,96]. Design variables in this research are cooling and heating setpoint temperature, insulation type, winter and summer clothing insulation level, insulation thickness, and insulation location. The purpose of designing these variables is to simultaneously reduce the H_L and C_L of the building and improve the T_c of the building's residents. The jEPlus software's generated design variables are displayed in Table 9.

According to topic 19 of Iran's national building laws and regulations [78], the temperature of the heating thermostat is 20 °C and the temperature of the cooling thermostat is 25 and 28 °C. In this study, to consider a larger range of this temperature, the temperature of the heating thermostat is set between 17 and 22.5 and the temperature of the cooling thermostat is set between 23 and 28.5 °C. The place of insulation is considered in three ways: inside, outside and middle. Insulation types available in the Iranian market have been used. These insulations are XPS, mineral wool, polyurethane, aerogel and cellulose. The thickness of the insulation has been chosen according to the size available in the market, which has the right price and dimensions. The clothing level is selected from 0 to 2. This value means that zero means that the residents of the building are not wearing any clothes, and the value of 2 means that the residents of the building use normal and very warm clothes inside the building. It is known that in the hot seasons of the year, this value is minimized and in the cold seasons of the year it should be maximized.

According to Table 8, the temperature of the heating-cooling thermostat has a direct effect on the cooling load. By increasing or decreasing these two inputs, the cooling and heating load of the building decreases. On the other hand, inappropriate temperature in different seasons causes thermal discomfort for the residents. Therefore, choosing the right heating thermostat temperature can have a significant impact on the three target functions.

The level of clothing of the residents for the two hot and cold seasons of the year causes the level of thermal comfort to vary. This is because one of the factors that determine the thermal comfort of the occupants is the level of clothing of the occupants. Other input factors are related to insulation, the changes of which affect the three objective functions.

3.2. MSA

Sensitivity analysis is a technique used by researchers to examine the impact of input variables on output variables. One of the many sensitivity analysis methods is the MSA [97]. OAT techniques, such as the MSA [97], only modify the value of one input parameter at a time. The MSA equations are as follows.

$$EE_i = \frac{f\left(X_1, \ldots, X_{i-1}, X_i + \Delta, X_{i+1}, \ldots, X_k\right) - f(X)}{\Delta} \tag{1}$$

$$\mu_i = \frac{1}{N}\sum_{r=1}^{n} EE_{i,r} \tag{2}$$

$$\sigma_i = \sqrt{\frac{1}{N-1}\sum_{r=1}^{n}\left(EE_{i,r} - \mu_i\right)^2} \tag{3}$$

According to Eqs. (2) and (3), the value needs to be higher the more the input parameter affects the output. Furthermore, as rises, greater improvements are made in the way that the input parameter interacts with other parameters.

3.3. Multi-objective optimization of H_L, C_L, and T_c

Lowering H_L and C_L while increasing T_c are the goals of the current research. Researchers' work in recent years has primarily focused on the investigation of workable ways to lower buildings' energy consumption. Reduced household energy use is becoming more crucial as electricity is generated in power stations by burning fossil fuels., which highlights the significance of this function. Numerous dangerous gases are released into the atmosphere as a result of increased electricity use and the burning of fossil fuels worldwide, endangering human life. Polluted air is delivered into a building through mechanical or natural ventilation, which lowers the quality of the indoor environment and endangers the health of the occupants. Therefore, a building with ideal specifications should be designed for the residential sector to lower energy consumption. There should be high heating comfort available to building occupants as well. Thus, a multi-objective optimization should be conducted to accomplish these objectives. It has been challenging for researchers to choose the appropriate optimization algorithms to apply to their research. As a result, they have examined their simulation results using a variety of optimization algorithms. One of the most popular algorithms for optimization is the genetic algorithm. A trustworthy algorithm in the field of multi-objective optimization is the Non-Dominant Genetic Algorithm (NSGA) [98], whose second iteration was published as NSGA-II in 2002 [25]. This algorithm has been applied in different sectors [99–102]. This study employs multi-objective optimization using the program JEPLUS EA [43]. JEPLUS parameterized data is required by software referred to as JEPLUS EA. The JEPLUS software is used to input both real-world and simulated data for optimization purposes. Following that, the JEPLUS software defines the design variables and uses these as inputs to reach the objective functions. Now, JEPLUS EA has received data that JEPLUS generated. Owing to the alternate interactions between the modes of the design variables, it encounters many modes. The model is then guided to the best points or Pareto front using the NSGA-II method. Population size, crossover rate, maximum number of generations, and mutation rate are all considered when configuring the algorithm, with the preliminary evaluation for convergence being performed at 20, 50, 100 %, and 20 %, respectively. After the optimization is finished and the NSGA-II algorithm generates the Pareto front, the best point must be chosen. It is possible to use a variety of statistical methods to find the most suitable solution. One beneficial technique frequently used by numerous researchers is the sum of the weighted method [103–105]. This approach determines the optimal response by using Eq (4).

$$f_{ws}(x) = \sum_{i=1}^{n} a_i \frac{f_i(x) - f_i(x)^{min}}{f_i(x)^{max} - f_i(x)^{min}} \tag{4}$$

Where $f_i(x)$ stands for the objectives, such as H_L, T_c, and C_L, and $f_i(x)^{max}$ and $f_i(x)^{min}$ stand for the highest and lowest values of every objective function, respectively. a_i is the weight correlation coefficient. Assuming that HL and CL are of equal importance results in the weight coefficient values of these two functions being set to the same value. Therefore, the weight coefficient can be determined using Eq (5).

$$a_2 = a_3 = \frac{1 - a_1}{2} \tag{5}$$

A multi-objective optimization issue was reduced to a single-objective optimization issue to find the coefficient a_1.

4. Result

Design variables' effects on objective functions can be demonstrated through statistical analysis, such as the MSA. Table 10 presents the sampling results from MSA for the design variables and objective functions [97].

According to Table 10, Clo_s and Clo_h only affect T_c and do not affect the other two objective functions. Also, it has the most influence on the H_L of the Hspt variable and the most influence on the C_L of the Cspt variable.

Before beginning the optimization, it is necessary to evaluate the preliminary values for the objective functions. The initial values of the objective functions for various cities are shown in Table 11 for this purpose.

After setting the initial parameters of the genetic algorithm, it is important that the parameters make the genetic algorithm converge. Fig. 6 shows the convergence diagram for the genetic algorithm. The green, blue, and red parts respectively show the number of population in each generation, the number of optimal points up to the current generation, and the number of optimal points found in each generation. According to Fig. 6, it can be seen that the optimization problem has reached a good convergence.

The user receives several points on the Pareto front from the JEPLUS + EA software after the optimization is completed. These points are not superior to one another because the opposing objective functions are also accounted for. To put it another way, neither of the other two objective functions are in their ideal states when one is. It is necessary to consider a point that satisfies all the objective functions. The sum of the weighted method is used as a result. Tc is impacted by the weight factor a_1, which has a range of 0–1. According to Eq. (5), the amount of T_c is at its maximum state and the states of the other two functions, H_L and C_L, are at their minimums when a_1 is zero. When the value of a_1 equals 1, on the other hand, T_c is at its highest point and the other objective functions are at their lowest points. The weight coefficient (a_1) is modified from 0 to 1 in steps of 0.1 to determine the optimal point. The best points are then identified. After that, one of the 11 optimal points that can satisfy all of the objective functions is picked. Tehran's Pareto optimal points are depicted in Fig. 7, and Table 12 elaborates on the properties of chosen Pareto front points for each weight coefficient value.

The T_c objective function is at its maximum value, while the H_L and C_L objective functions are at their minimum values, as shown in Table 12 when the weighting coefficient is zero. As the weighting factor increases, the value of the other objective function falls, whereas increasing the weighting factor raises the value of the two other objective functions with the same coefficients. As it reaches 1, the other two functions have zero weighting coefficients, which negates their influence on the best choice. The objective function measuring Tc is therefore at its minimum point at this time, while the other two objective functions are at their maximum points. It seems that the point with the weight factor value of 0.5 is the most suitable point among the 12 ideal states. The reason for the selection is that the values of H_L and C_L are reduced to a suitable value. Also, if we add the cooling and heating load together, it has a lower annual load. As an example, the annual load for the weighting factor of 0.4, 0.5 and 0.6 is equal to 16980 kWh, 15657 kWh and 18403 kWh. Also, if the PPD (T_c) value is close to 10 %, it is optimal, and the value of the weight coefficient is 0.5 times 12 %, which indicates the appropriate thermal comfort.

Table 12 and Fig. 8 demonstrate that increasing the thermostat's heating temperature causes a significant rise in H_L. Before increasing, the value of T_C first falls to 19.5°. There is no set pattern for the C_L. Because of Tehran's climate, the air conditioning system has to consume more electricity to raise the thermostat's heating temperature and create the desired room temperature. A temperature that can fulfill all three objective functions ought to be taken into account. At a temperature of 18 °C, the objective functions of the present study are suitably optimized. Moreover, the C_L decreases as the cooling temperature rises. When the temperature reaches 26°, the value of T_C first starts to rise. A suitable value for the H_L is between 25 and 26. 5°. As a result, all three of the thermostat's intended functions are almost completely satisfied by cooling temperatures above 25 °C. Tehran has a mildly cold climate, so the air conditioner doesn't produce as much cold air. Furthermore, with the rise in thermostat temperature, less C_L is needed to maintain a comfortable indoor temperature. Fig. 9 demonstrates that the thermostat's cooling temperature of 26.5 (°C) yields the most ideal results for the three objective functions.

According to Fig. 10, it can be seen that the changes of the I_p are noticeable in the three objective functions, for the C_L and T_c, the value of the outside location is lower than the others, and for the H_L, the middle location has the lowest value. In general, the best I_p for Tehran is outside.

According to Fig. 11, as expected, insulation with lower thermal conductivity prevented more heat loss of the building and the C_L and H_L of aerogel insulation has the lowest value. The C_L and H_L increase as the thermal conductivity coefficient increases. For T_c, this difference is very minor and small, and all insulations are close to each other in the lowest amount of T_c.

According to Fig. 12, it can be seen that the behavior of Tc with the I_{th} first decreased and then increased. This pattern first decreased to a thickness of 6 cm and then increased. One of the reasons for this pattern can be because the space stays too hot in the summer season, which disturbs the T_c of the residents. For the HL of this pattern, it decreases from 1 cm to 8 cm and increases from 8 cm to 10 cm. For the C_L, it does not follow a specific trend and its value decreases and increases for various thicknesses, but in the thickness range between 7 and 8 cm, the cooling load is relatively less. With these interpretations, the optimal value of I_{th} is equal to 8 cm.

Figs. 13 and 14 show the values of the changes in the residents' summer clothes. According to the sensitivity analysis performed in the previous stages, the changes in the Clo_w and Clo_s do not affect the C_L and H_L only affects the T_c. However, it can be seen that the surface value of Clo_s up to 1.2 decreases the T_c (improving the T_c of the residents) and after that the T_c increases or it can be said that the T_c of the residents is disturbed. It is the same for the Clo_w, it decreases from 0 to 1.6 and improves the T_c of the residents, and from 1.6 onwards, it increases the T_c and disturbs the T_c of the residents. According to these values, the best values for Clo_s and Clo_w are 0.8 and 1.45, respectively.

The same process is done for the other three cities. Fig. 15 and Table 13 show the optimal points of the front beam for 4 cities. The results show that the best temperature for the hspt is 18 °C and the cspt is between 26.5 and 27.5 °C. The best I_t is aerogel insulation, and it is also the best place for outside and inside insulation. I_{th} between 8 and 9.5 cm is optimal for all cities. Finally, Clo_s and Clo_w are the lowest for warm cities like Bandar Abbas and the highest for cold cities like Tabriz.

According to Fig. 16, the value of T_c, H_L, and C_L has improved between 38 and 62, 61 to 100, and 17–39 %, respectively. The highest T_c improvement is related to Rasht city and the lowest improvement is related to Bandar Abbas City. The highest H_L improvement is related to Bandar Abbas city and the lowest improvement is related to Tabriz city. The highest C_L improvement is related to Bandar Abbas city and the lowest improvement is related to Rasht city.

5. Conclusions

In this article, the goal is to improve T_c along with reducing the H_L and C_L of the building. For this purpose, seven design variables were selected. Using the NSGA-II algorithm, optimization was done for four cities with different climates, and the results are as follows.

- According to the Morris sensitivity analysis, Clo_s and Clo_h only affect T_c and do not affect the other two objective functions. It also has the greatest effect on the H_L of the Hspt variable and the greatest effect on the C_L of the Cspt variable.
- The results showed that the best temperature for all cities is hspt 18 °C and cspt between 26.5 and 27.5 °C.
- Among the 6 selected insulations, the best type of insulation is aerogel insulation. This is because this insulation has a lower thermal conductivity and prevents excessive heat loss from the building.

- The results showed that for the cities that have the biggest temperature difference between night and day, such as Bandar Abbas and Tabriz, the greatest thickness of insulation is required in the building, and the cities of Tehran and Rasht, which are less than these two cities, require less insulation thickness. According to the results, this thickness has been chosen to be 8 cm for Rasht and Tehran and 9 and 9.5 cm for Tabriz and Bandar Abbas cities.
- The cities of Bandar Abbas, Tabriz and Tehran receive the most solar radiation. But the city of Rasht receives less solar radiation due to being close to the sea level and far from the equator. For the city of Rasht, which receives less solar radiation, the best place to insulate is inside, and this is because there is little radiant heat inside the space and it must be kept so that there is less loss. For the other three cities, the best insulation position is outside.
- Due to the coldness of the city of Tabriz, the level of clothing for the winter of this city is the highest and is equal to 1.9. This value is the lowest value for the city of Bandar Abbas, which is warm and equal to 0.6. Also, for the level of clothing for summer, these values are 1.15 and 0.2 for Tabriz and Bandar Abbas, respectively.
- The highest heating load is related to the city of Tabriz and is equal to 14370.9 kWh and the highest cooling load is related to the city of Band Abbas and is equal to 30131 kWh.
- The lowest heating load corresponds to the city of Bandar Abbas and is equal to 0.84 kWh, and the lowest cooling load corresponds to the city of Tabriz and is equal to 3644.11 kWh.
- According to the result, T_c, H_L, and C_L values improved by 38–62, 61 to 100, and 17 to 39 percent, respectively.

Future study, limitation and suggestions

The time step is one of the study's drawbacks. Energy software's suggested time step is 20, which is what this study uses. However, the simulation result improves somewhat when the time step is increased to 60. However, there is a significant increase in calculating time, which is not cost-effective. For future studies, economic analysis can be done along with cooling and heating loads, so that it can be an important choice for architectural engineers. In most of the real scenarios, first one parameter is brought to the optimum point and then next parameters are studied one by one and their effects on output is checked. This process causes the work to be time-consuming and expensive. But in cases where multi-objective optimization is used, it has the advantage of observing the effect of several parameters on several outputs at the same time, leaving the designer multiple choice to choose based on design priorities.

CRediT authorship contribution statement

Mohammadreza Baghoolizadeh: Supervision, Writing – review & editing, Conceptualization, Data curation, Formal analysis. **Mahmoud Behzadi Hamooleh:** Supervision, Writing – review & editing, Conceptualization, Data curation, Formal analysis. **As'ad Alizadeh:** Formal analysis, Data curation, Conceptualization. **Amir Torabi:** Writing – review & editing, Conceptualization, Data curation, Formal analysis. **Dheyaa J. Jasim:** Supervision, Writing – review & editing, Conceptualization, Data curation, Formal analysis. **Mohammad Rostamzadeh-Renani:** Investigation, Writing – original draft. **Reza Rostamzadeh-Renani:** Investigation, Writing – original draft.

Declaration of competing interest

The authors declare that they have no known competing financial interests or personal relationships that could have appeared to influence the work reported in this paper.

Data availability

No data was used for the research described in the article.

References

[1] E. Bellos, et al., Energetic and financial evaluation of solar assisted heat pump space heating systems, Energy Convers. Manag. 120 (2016) 306–319.
[2] A.M. Khudhair, M.M. Farid, A review on energy conservation in building applications with thermal storage by latent heat using phase change materials, Energy Convers. Manag. 45 (2) (2004) 263–275.
[3] Climate Plan, L.s.a.t.t.c.o.c.c, Technical Report French Ministry of Ecology and Sustainable Development, 2004.
[4] K.K. Wan, et al., Future trends of building heating and cooling loads and energy consumption in different climates, Build. Environ. 46 (1) (2011) 223–234.
[5] IEA. IEA statistics, World energy statistics and balances, http://www.iea.org/statistics-/topics/energybalances/, 2014.
[6] M. Khoukhi, The combined effect of heat and moisture transfer dependent thermal conductivity of polystyrene insulation material: impact on building energy performance, Energy Build. 169 (2018) 228–235.
[7] U. Berardi, A cross-country comparison of the building energy consumptions and their trends, Resour. Conserv. Recycl. 123 (2017) 230–241.
[8] G. Bakos, Insulation protection studies for energy saving in residential and tertiary sector, Energy Build. 31 (3) (2000) 251–259.
[9] D. Chwieduk, Towards sustainable-energy buildings, Appl. Energy 76 (1–3) (2003) 211–217.
[10] M. Bojic, F. Yik, P. Sat, Influence of thermal insulation position in building envelope on the space cooling of high-rise residential buildings in Hong Kong, Energy Build. 33 (6) (2001) 569–581.
[11] A. Bolattürk, Optimum insulation thicknesses for building walls with respect to cooling and heating degree-hours in the warmest zone of Turkey, Build. Environ. 43 (6) (2008) 1055–1064.
[12] M.A. Aktacir, O. Büyükalaca, T. Yılmaz, A case study for influence of building thermal insulation on cooling load and air-conditioning system in the hot and humid regions, Appl. Energy 87 (2) (2010) 599–607.
[13] M. Ozel, Determination of optimum insulation thickness based on cooling transmission load for building walls in a hot climate, Energy Convers. Manag. 66 (2013) 106–114.
[14] J. Yu, et al., A study on optimum insulation thicknesses of external walls in hot summer and cold winter zone of China, Appl. Energy 86 (11) (2009) 2520–2529.
[15] M.K. Nematchoua, et al., Study of the economical and optimum thermal insulation thickness for buildings in a wet and hot tropical climate: case of Cameroon,

Renew. Sustain. Energy Rev. 50 (2015) 1192–1202.
[16] F.F.C. Vincelas, T. Ghislain, The determination of the most economical combination between external wall and the optimum insulation material in Cameroonian's buildings, J. Build. Eng. 9 (2017) 155–163.
[17] X. Liu, et al., Determination of optimum insulation thickness for building walls with moisture transfer in hot summer and cold winter zone of China, Energy Build. 109 (2015) 361–368.
[18] M.F. Alsayed, R.A. Tayeh, Life cycle cost analysis for determining optimal insulation thickness in Palestinian buildings, J. Build. Eng. 22 (2019) 101–112.
[19] M. Shekarchian, et al., The cost benefit analysis and potential emission reduction evaluation of applying wall insulation for buildings in Malaysia, Renew. Sustain. Energy Rev. 16 (7) (2012) 4708–4718.
[20] N. Daouas, Z. Hassen, H.B. Aissia, Analytical periodic solution for the study of thermal performance and optimum insulation thickness of building walls in Tunisia, Appl. Therm. Eng. 30 (4) (2010) 319–326.
[21] D. D'Agostino, et al., Proposal of a new automated workflow for the computational performance-driven design optimization of building energy need and construction cost, Energy Build. 239 (2021) 110857.
[22] T. Tzoulis, K. Kontoleon, Thermal behaviour of concrete walls around all cardinal orientations and optimal thickness of insulation from an economic point of view, Procedia environmental sciences 38 (2017) 381–388.
[23] M. Baghoolizadeh, et al., A multi-objective optimization of a building's total heating and cooling loads and total costs in various climatic situations using response surface methodology, Energy Rep. 7 (2021) 7520–7538.
[24] M. Baghoolizadeh, et al., Optimization of annual electricity consumption costs and the costs of insulation and phase change materials in the residential building using artificial neural network and genetic algorithm methods, J. Energy Storage 62 (2023) 106916.
[25] K. Deb, et al., A fast and elitist multiobjective genetic algorithm: NSGA-II, IEEE Trans. Evol. Comput. 6 (2) (2002) 182–197.
[26] P Preethi, H.R. Mamatha, Region-based convolutional neural network for segmenting text in epigraphical images, Artif, Intell. Appl. 1 (2) (2023) 119–127, https://doi.org/10.47852/bonviewAIA2202293.
[27] T. Peng, et al., Geometric prior guided hybrid deep neural network for facial beauty analysis, CAAI Trans. Intell. Technol. (2023) 1–14. https://doi.org/10.1049/cit2.12197.
[28] J. Chen, Z. Wang, C.-L. Liu, Lateral interaction by Laplacian-based graph smoothing for deep neural networks, CAAI Trans. Intell. Technol. 8 (4) (2023) 1590–1607. https://doi.org/10.1049/cit2.12265.
[29] L. Zhao, et al., The dynamic relaxation form finding method aided with advanced recurrent neural network, CAAI Trans. Intell. Technol. 8 (3) (2023) 635–644. https://doi.org/10.1049/cit2.12177.
[30] C. Xi, J. Yang, X. Liang, R. Bin Ramli, S. Tian, G. Feng, D. Zhen, An improved gatedconvolutional neural network for rolling bearing fault diagnosis with imbalanced data, Int. J. Hydromechatron. 6 (2) (2023) 108–132.
[31] S.L.H. Lau, J. Lim, E.K.P. Chong, X. Wang, Single-pixel image reconstruction based on block compressive sensing and convolutional neural network, Int. J. Hydromechatronics 6 (3) (2023) 258–273.
[32] M. Baghoolizadeh, et al., Prediction and extensive analysis of MWCNT-MgO/oil SAE 50 hybrid nano-lubricant rheology utilizing machine learning and genetic algorithms to find ideal attributes, Tribol. Int. (2024) 109582.
[33] M. Rostamzadeh-Renani, et al., A multi-objective and CFD based optimization of roof-flap geometry and position for simultaneous drag and lift reduction, Propulsion and Power Research 13 (1) (2024) 26–45.
[34] M. Baghoolizadeh, et al., Using of artificial neural networks and different evolutionary algorithms to predict the viscosity and thermal conductivity of silica-alumina-MWCN/water nanofluid, Heliyon 10 (4) (2024) e26297.
[35] R. Rostamzadeh-Renani, et al., Multi-objective optimization of rheological behavior of nanofluids containing CuO nanoparticles by NSGA II, MOPSO, and MOGWO evolutionary algorithms and Group Method of Data Handling Artificial neural networks, Mater. Today Commun. 38 (2024) 107709.
[36] M. Bayareh, M. Baghoolizadeh, An overview of the magnetic field effect on heat transfer and entropy generation in cavities: application of the second law of thermodynamics and artificial intelligence, Int. Commun. Heat Mass Tran. 151 (2024) 107238.
[37] M. Baghoolizadeh, et al., Using different machine learning algorithms to predict the rheological behavior of oil SAE40-based nano-lubricant in the presence of MWCNT and MgO nanoparticles, Tribol. Int. 187 (2023) 108759.
[38] R. Rostamzadeh-Renani, et al., Prediction of the thermal behavior of multi-walled carbon nanotubes-CuO-CeO2 (20-40-40)/water hybrid nanofluid using different types of regressors and evolutionary algorithms for designing the best artificial neural network modeling, Alex. Eng. J. 84 (2023) 184–203.
[39] M. Rostamzadeh-Renani, et al., The effect of vortex generators on the hydrodynamic performance of a submarine at a high angle of attack using a multi-objective optimization and computational fluid dynamics, Ocean. Eng. 282 (2023) 114932.
[40] M. Baghoolizadeh, et al., Improving CO2 concentration, CO2 pollutant and occupants' thermal comfort in a residential building using genetic algorithm optimization, Energy Build. 291 (2023) 113109.
[41] M. Baghoolizadeh, et al., Multi-objective optimization of annual electricity consumption and annual electricity production of a residential building using photovoltaic shadings, Int. J. Energy Res. 46 (15) (2022) 21172–21216.
[42] M. Baghoolizadeh, et al., Multi-objective optimization of Venetian blinds in office buildings to reduce electricity consumption and improve visual and thermal comfort by NSGA-II, Energy Build. 278 (2023) 112639.
[43] Y. Zhang, Use jEPlus as an efficient building design optimisation tool, in: CIBSE ASHRAE Technical Symposium, Imperial College London, 2012.
[44] Y. Zhai, et al., A multi-objective optimization methodology for window design considering energy consumption, thermal environment and visual performance, Renew. Energy 134 (2019) 1190–1199.
[45] E. Naderi, et al., Multi-objective simulation-based optimization of controlled blind specifications to reduce energy consumption, and thermal and visual discomfort: case studies in Iran, Build. Environ. 169 (2020) 106570.
[46] N. Delgarm, et al., A novel approach for the simulation-based optimization of the buildings energy consumption using NSGA-II: case study in Iran, Energy Build. 127 (2016) 552–560.
[47] H. Sghiouri, A. Mezrhab, H. Naji, Overhangs' optimization of a southsouth-facing residential building in semi-arid climate, in: 2017 International Renewable and Sustainable Energy Conference (IRSEC), IEEE, 2017.
[48] R.D. Bingham, M. Agelin-Chaab, M.A. Rosen, Whole building optimization of a residential home with PV and battery storage in the Bahamas, Renew. Energy 132 (2019) 1088–1103.
[49] O.T. Karaguzel, R. Zhang, K.P. Lam, Coupling of whole-building energy simulation and multi-dimensional numerical optimization for minimizing the life cycle costs of office buildings, in: Building Simulation, Springer, 2014.
[50] A. Baniassadi, et al., Economic optimization of PCM and insulation layer thickness in residential buildings, Sustain. Energy Technol. Assessments 14 (2016) 92–99.
[51] E. BellosC T, A. Kouvari, K.A. Antonopoulos, Comparison of heating and cooling loads of a typical building with TRNSYS and eQUEST, in: Energy, Transportation and Global Warming, Springer, Cham, 2016, pp. 327–338, https://doi.org/10.1007/978-3-319-30127-3_25.
[52] E. Solgi, S. Memarian, G.N. Moud, Financial viability of PCMs in countries with low energy cost: a case study of different climates in Iran, Energy Build. 173 (2018) 128–137.
[53] G. Mitsopoulos, E. Bellos, C. Tzivanidis, Financial and energetic optimization of Greek buildings insulation, Design 2 (3) (2018) 34.
[54] E. Markarian, F. Fazelpour, Multi-objective optimization of energy performance of a building considering different configurations and types of PCM, Sol. Energy 191 (2019) 481–496.
[55] S. Çağlayan, et al., A life cycle costing approach to determine the optimum insulation thickness of existing buildings, Isı Bilimi ve Tekniği Dergisi 40 (1) (2020) 1–14.
[56] Y. Wang, B. Li, W. Zheng, Optimum insulation thickness for the sandwich structure livestock buildings external envelopes in different climate regions of China, Int. J. Agric. Biol. Eng. 13 (1) (2020) 29–41.
[57] H. Huang, et al., Optimum insulation thicknesses and energy conservation of building thermal insulation materials in Chinese zone of humid subtropical

climate, Sustain. Cities Soc. 52 (2020) 101840.
[58] R.A. Kishore, et al., Optimizing PCM-integrated walls for potential energy savings in US Buildings, Energy Build. 226 (2020) 110355.
[59] B. Rosti, A. Omidvar, N. Monghasemi, Optimal insulation thickness of common classic and modern exterior walls in different climate zones of Iran, J. Build. Eng. 27 (2020) 100954.
[60] N. Aydin, A. Biyikoğlu, Determination of optimum insulation thickness by life cycle cost analysis for residential buildings in Turkey, Science and Technology for the Built Environment 27 (1) (2021) 2–13.
[61] M.A. Kallioğlu, et al., Optimum insulation thickness assessment of different insulation materials for mid-latitude steppe and desert climate (BSH) region of India, Mater. Today: Proc. 44 (2021) 4421–4424.
[62] E. Küçüktopcu, B. Cemek, The use of artificial neural networks to estimate optimum insulation thickness, energy savings, and carbon dioxide emissions, Environ. Prog. Sustain. Energy 40 (1) (2021) e13478.
[63] R. Dylewski, J. Adamczyk, Optimum thickness of thermal insulation with both economic and ecological costs of heating and cooling, Energies 14 (13) (2021) 3835.
[64] A.E. Akan, Determination and modeling of optimum insulation thickness for thermal insulation of buildings in all city centers of Turkey, Int. J. Thermophys. 42 (4) (2021) 1–34.
[65] H. Bagheri-Esfeh, M.R. Dehghan, Multi-objective optimization of setpoint temperature of thermostats in residential buildings, Energy Build. 261 (2022) 111955.
[66] L. Wen, K. Hiyama, A review: simple tools for evaluating the energy performance in early design stages, Procedia Eng. 146 (2016) 32–39.
[67] C. Underwood, An improved lumped parameter method for building thermal modelling, Energy Build. 79 (2014) 191–201.
[68] B. Pandey, R. Banerjee, A. Sharma, Coupled EnergyPlus and CFD analysis of PCM for thermal management of buildings, Energy Build. 231 (2021) 110598.
[69] B. Shen, J. New, V. Baxter, Air source integrated heat pump simulation model for EnergyPlus, Energy Build. 156 (2017) 197–206.
[70] R. Zhang, et al., Coupled EnergyPlus and computational fluid dynamics simulation for natural ventilation, Build. Environ. 68 (2013) 100–113.
[71] S. Andolsun, et al., EnergyPlus vs. DOE-2.1 e: The effect of ground-coupling on energy use of a code house with basement in a hot-humid climate, Energy Build. 43 (7) (2011) 1663–1675.
[72] N. Queiroz, F.S. Westphal, F.O.R. Pereira, A performance-based design validation study on EnergyPlus for daylighting analysis, Build. Environ. 183 (2020) 107088.
[73] N.M. Mateus, A. Pinto, G.C. Da Graça, Validation of EnergyPlus thermal simulation of a double skin naturally and mechanically ventilated test cell, Energy Build. 75 (2014) 511–522.
[74] H. Du, J. Edge, C. Underwood, Modelling the Impacts of New UK Future Weather Data on a School Building, 2011.
[75] P. Pourvahidi, M.B. Ozdeniz, Bioclimatic analysis of Iranian climate for energy conservation in architecture, Sci. Res. Essays 8 (1) (2013) 6–16.
[76] https://energyplus.net/weather-region/asia_wmo_region_2/IRN.
[77] https://climate.onebuilding.org/WMO_Region_2_Asia/IRN_Iran/index.html. Site to view weather data. Seen at 11 November 2022; Available from: https://climate.onebuilding.org/WMO_Region_2_Asia/IRN_Iran/index.html.
[78] Code No.19E.E., Bureau for compiling and promoting national regulations for buildings, Ministry of Housing and Urbanism (2011) (In Persian).
[79] Code No.19: Energy Efficiency Bureau for compiling and promoting National regulations for Buildings, Ministry of Housing and Urbanism. 2011: Tehran, Iran.
[80] National Building Code, Part 13 Design and Implementation of Electrical Installations for Buildings, Iran Building and Housing Research Center, Tehran, Iran, 2009.
[81] Help_EnergyPlus.
[82] K. Muruganantham, Application of Phase Change Material in Buildings: Field Data vs. EnergyPlus Simulation, Arizona State University, 2010.
[83] H. Bagheri-Esfeh, H. Safikhani, S. Motahar, Multi-objective optimization of cooling and heating loads in residential buildings integrated with phase change materials using the artificial neural network and genetic algorithm, J. Energy Storage 32 (2020) 101772.
[84] A. Fathalian, H. Kargarsharifabad, Actual validation of energy simulation and investigation of energy management strategies (Case Study: an office building in Semnan, Iran), Case Stud. Therm. Eng. 12 (2018) 510–516.
[85] P.C. Tabares-Velasco, et al., Verification and Validation of EnergyPlus Conduction Finite Difference and Phase Change Material Models for Opaque Wall Assemblies, National Renewable Energy Lab.(NREL), Golden, CO (United States), 2012.
[86] W. Pereira, A. Bögl, T. Natschläger, Sensitivity analysis and validation of an EnergyPlus model of a house in Upper Austria, Energy Proc. 62 (2014) 472–481.
[87] R.H. Henninger, M.J. Witte, D.B. Crawley, Analytical and comparative testing of EnergyPlus using IEA HVAC BESTEST E100–E200 test suite, Energy Build. 36 (8) (2004) 855–863.
[88] R. Kamal, et al., Strategic control and cost optimization of thermal energy storage in buildings using EnergyPlus, Appl. Energy 246 (2019) 77–90.
[89] Mashrae, Y.Z.P., Use jEPlus as an Efficient Building Design Optimisation Tool.
[90] Y. Zhang, I. Korolija, Performing complex parametric simulations with jEPlus, in: SET2010-9th International Conference on Sustainable Energy Technologies, 2010.
[91] E. Naboni, et al., Extending the use of parametric simulation in practice through a cloud based online service, in: IBPSA Italy-Conference of International Building Performance Simulation Association, 2013 *Bozen, Italy*.
[92] X. Chen, H. Yang, K. Sun, A holistic passive design approach to optimize indoor environmental quality of a typical residential building in Hong Kong, Energy 113 (2016) 267–281.
[93] S. Naji, L. Aye, M. Noguchi, Sensitivity analysis on energy performance, thermal and visual discomfort of a prefabricated house in six climate zones in Australia, Appl. Energy 298 (2021) 117200.
[94] N. Delgarm, et al., Sensitivity analysis of building energy performance: a simulation-based approach using OFAT and variance-based sensitivity analysis methods, J. Build. Eng. 15 (2018) 181–193.
[95] R. Chen, Y.-S. Tsay, An integrated sensitivity analysis method for energy and comfort performance of an office building along the Chinese coastline, Buildings 11 (8) (2021) 371.
[96] R. Guo, et al., Influence of design parameters on the night ventilation performance in office buildings based on sensitivity analysis, Sustain. Cities Soc. 50 (2019) 101661.
[97] M.D. Morris, Factorial sampling plans for preliminary computational experiments, Technometrics 33 (2) (1991) 161–174.
[98] Y. Yusoff, M.S. Ngadiman, A.M. Zain, Overview of NSGA-II for optimizing machining process parameters, Procedia Eng. 15 (2011) 3978–3983.
[99] J. Rui, H. Yao, Parallel test task scheduling based on improved adaptive genetic algorithm, J. Ord. Equip. Eng. 44 (9) (2023) 298–305.
[100] C. Jiahang, L. Jianghong, Z. Wei, et al., Research on high altitude simulation test of aero engine based on genetic algorithm optimization uniform design, J. Ord. Equip. Eng. 44 (9) (2023) 285–289.
[101] F. Rosso, et al., Multi-objective optimization of building retrofit in the Mediterranean climate by means of genetic algorithm application, Energy Build. 216 (2020) 109945.
[102] M.-D. Yang, et al., Multiobjective optimization using nondominated sorting genetic algorithm-II for allocation of energy conservation and renewable energy facilities in a campus, Energy Build. 122 (2016) 120–130.
[103] N. Delgarm, B. Sajadi, S. Delgarm, Multi-objective optimization of building energy performance and indoor thermal comfort: a new method using artificial bee colony (ABC), Energy Build. 131 (2016) 42–53.
[104] M. Karmellos, A. Kiprakis, G. Mavrotas, A multi-objective approach for optimal prioritization of energy efficiency measures in buildings: model, software and case studies, Appl. Energy 139 (2015) 131–150.
[105] J.-h. Ryu, S. Kim, H. Wan, Pareto front approximation with adaptive weighted sum method in multiobjective simulation optimization, in: Proceedings of the 2009 Winter Simulation Conference (WSC), IEEE, 2009.